Published OnlineFirst September 14, 2010; DOI:10.1158/0008-5472.CAN-09-4360

Cancer Research

Image-Based Chemical Screening Identifies Drug Efflux Inhibitors in Lung Cancer Cells

Xiaofeng Xia, Jian Yang, Fuhai Li, et al.

Cancer Res 2010;70:7723-7733. Published OnlineFirst September 14, 2010.

Published OnlineFirst September 14, 2010; DOI:10.1158/0008-5472.CAN-09-4360

Tumor and Stem Cell Biology

Cancer Research

Image-Based Chemical Screening Identifies Drug Efflux Inhibitors in Lung Cancer Cells

Xiaofeng Xia[1], Jian Yang[1], Fuhai Li[1], Ying Li[2], Xiaobo Zhou[1], Yue Dai[2], and Stephen T.C. Wong[1]

Abstract

Cancer cells with active drug efflux capability are multidrug resistant and pose a significant obstacle for the efficacy of chemotherapy. Moreover, recent evidence suggests that high drug efflux cancer cells (HDECC) may be selectively enriched with stem-like cancer cells, which are believed to be the cause for tumor initiation and recurrence. There is a great need for therapeutic reagents that are capable of eliminating HDECCs. We developed an image-based high-content screening (HCS) system to specifically identify and analyze the HDECC population in lung cancer cells. Using the system, we screened 1,280 pharmacologically active compounds that identified 12 potent HDECC inhibitors. It is shown that these inhibitors are able to overcome multidrug resistance (MDR) and sensitize HDECCs to chemotherapeutic drugs, or directly reduce the tumorigenicity of lung cancer cells possibly by affecting stem-like cancer cells. The HCS system we established provides a new approach for identifying therapeutic reagents overcoming MDR. The compounds identified by the screening may potentially be used as potential adjuvant to improve the efficacy of chemotherapeutic drugs. *Cancer Res; 70(19); 7723–33. ©2010 AACR.*

Introduction

Multidrug-resistant cancer cells often survive chemotherapy and lead to tumor relapse. One of the most common mechanisms underlying multidrug resistance (MDR) is drug efflux, mediated by the ATP-binding cassette (ABC) transporters overexpressed on the cell membrane, which act as efflux pumps to transport the drugs outwards (1, 2). Overcoming MDR by inhibiting the ABC transporters has been unsuccessful, with three generations of inhibitors developed and subjected to clinical trials but few significant advances made (3–5). Intolerable side effects were frequently observed as a result of the multiple pharmacologic activities of the inhibitors. Pharmacokinetic interactions were often induced that limited the clearance and metabolism of the coadministered chemotherapeutic drugs (5). These results suggest that direct inhibition of ABC transporters may not be the ideal strategy to combat MDR and alternative approaches are needed to eliminate the drug efflux cancer cells.

A large degree of heterogeneity has been observed in the drug efflux capability for cancer cells within the same tumor. Eliminating the cells with high drug efflux capability is particularly important, as they are more likely to survive chemotherapy and lead to tumor relapse. More interestingly, substantial evidences from many independent labs suggest that the high drug efflux cancer cell (HDECC) population may be highly enriched for stem-like cancer cells (6–14), which are believed to be the cause of tumor initiation, propagation, and recurrence (15–17). Therefore, therapeutic treatment eliminating HDECCs may help to remove stem-like cancer cells and prevent tumor relapse. This further highlights the importance of the development of therapeutic reagent specifically targeting HDECCs.

Drug discovery on HDECCs has been impeded by the lack of appropriate high-throughput techniques. HDECCs have been identified and isolated by flow cytometry, mostly using the side population (SP) technique (18). However, the application of the flow cytometry approach in high-throughput studies is restrictive, as it requires cumbersome single-cell dissociation and the throughput of the instrument itself is rather low. To date, there is no report of high-throughput studies using the SP technique. On the other hand, recently, automated image analysis aided by high-performance computing has enabled rapid advances in the development of high-throughput image-based assays (19–22). Considering that the fluorescence variance indicating HDECCs in SP technique can be readily detected by fluorescence microscopy, we sought to develop a new assay to identify and analyze HDECCs based on fluorescence images. Compared with flow cytometry, the image-based assay can be carried out directly on attached live cells so that high throughput is easily achievable with a regular automated fluorescence microscope. Direct visualization of the cellular phenotype also permits more comprehensive measurements of the responses to

Authors' Affiliations: [1]Medical Systems Biology Laboratory, Center for Bioengineering and Informatics, The Methodist Hospital Research Institute, Weill Cornell Medical College, Houston, Texas and [2]Department of Chinese Pharmacology, China Pharmaceutical University, Nanjing, Jiangsu, People's Republic of China

Note: Supplementary data for this article are available at Cancer Research Online (http://cancerres.aacrjournals.org/).

Corresponding Author: Stephen T.C. Wong, Department of Radiology, The Methodist Hospital, B5-022, Houston, TX 77030. Phone: 713-441-5884; Fax: 713-441-8699; E-mail: stwong@tmhs.org.

doi: 10.1158/0008-5472.CAN-09-4360

Published OnlineFirst September 14, 2010; DOI:10.1158/0008-5472.CAN-09-4360

perturbations, and the measurements can be performed specifically on single cells of interest (22). Moreover, considering the wide availability of fluorescence microscopes, development of such image-based assay will greatly accelerate related research by allowing faster and cheaper collection of high-throughput data, which may lead to novel treatment against MDR or even cancer stem cells.

In this study, we first established a high-content screening (HCS; ref. 23) system based on an image-based assay, which can identify and analyze HDECCs. Using the system, we screened 1,280 pharmacologically active compounds for their effect on the prevalence of HDECCs in lung cancer cells. The screening successfully identified compounds capable of turning HDECCs into non-HDECCs by removing their drug efflux capability, and we named them HDECC inhibitors. It is shown that these inhibitors can significantly enhance the efficacy of chemotherapeutic drugs or reduce the tumorigenicity of cancer cells. These results support a correlation of the HDECC population with stem-like cancer cells and suggest that better therapeutic effect may be achieved by removing the population. The compounds identified not only have the potential to be used as drugs to improve chemotherapy efficacy but also provide insight into the possible mechanism underlying the biology of HDECCs.

Materials and Methods

Cell lines and compounds

All the cell lines were purchased from the American Type Culture Collection (ATCC) and grown in DMEM with 10% fetal bovine serum (FBS) and penicillin/streptomycin at 37°C in a humidified incubator with 5% CO_2, and they were used within 10 passages for <6 months after receipt. Cell lines were characterized by ATCC by morphology check, growth curve analysis, and short tandem repeat DNA profiling. After receipt, cells were confirmed to be free from *Mycoplasma* contamination using the Mycoplasma Detection kit (Roche Applied Science). Library of pharmacologically active compounds (LOPAC) was purchased from Sigma-Aldrich.

Image-based assay

Cancer cells were first incubated with 5 μg/mL Hoechst 33342 for 90 minutes at 37°C to stain the cell nuclei. Fluorescence images were taken using a 4′,6-diamidino-2-phenylindole filter to measure the intensity of each nucleus. After that, verapamil was added to the medium to a final concentration of 50 μmol/L to block the efflux pump, and the fluorescence intensities of the nuclei were monitored for 30 minutes by time-lapse imaging. The experiments were carried out on an Olympus FV1000 microscope. Images were taken using an Olympus UPlanFL 4×/0.13 PhP objective and analyzed with a customized DCellIQ software with details described in Supplementary Materials and Methods.

Flow cytometry

Cells were treated with indicated compound for 48 hours and subjected to SP analysis using the methods described by Goodell and colleagues (18) with modifications. Briefly, cells were dissociated with trypsin-EDTA to single cells and resuspended at 1×10^6/mL in prewarmed DMEM with 2% FBS and 10 mmol/L HEPES. They were stained with 5 μg/mL Hoechst 33342 for 90 minutes at 37°C, then washed with ice-cold HBSS with 2% FBS and 10 mmol/L HEPES once, and resuspended in the same buffer with 2 μg/mL propidium iodide to gate viable cells. The cells were filtered through a 40-μm cell strainer to obtain single-cell suspension before they were sorted by flow cytometry. Analysis and sorting were done on a MoFlo cell sorter (Dako). The Hoechst 33342 dye was excited at 357 nm, and its fluorescence was analyzed under dual wavelength of 402 to 446 nm (blue) and 650 to 670 nm (red).

Cytotoxicity assay

SP cells isolated by flow cytometry were counted and seeded in 96-well plate at 2×10^4 per well. Cells were allowed to recover for 24 hours before the assay. To test the cytotoxicity of the compound alone, cells were treated with 5 μmol/L of the indicated compound. For *in vitro* chemotherapy efficiency test, cells were treated with four different chemotherapeutic drugs at the following concentrations: cisplatin, 100 μmol/L; etoposide, 100 μmol/L; doxorubicin, 20 μmol/L; paclitaxel, 400 nmol/L, with indicated compound at 5 μmol/L or vehicle (0.05% DMSO). Cell viability was measured 48 hours later using colorimetric MTS cell proliferation assay (CellTiter 96 Aqueous Non-Radioactive Cell Proliferation Assay, Promega). Absorbance was measured at 490 nm with a microplate reader (FluoStar Optima). Background was corrected using an empty well as a control. Cytotoxicity was calculated as follows:

$$\text{Cytotoxicity } (\%) = \frac{(\text{OD}_{\text{untreated well}} - \text{OD}_{\text{treated well}})}{\text{OD}_{\text{untreated well}}} \times 100$$

Tumor xenograft

Animals were purchased from Charles River, and experiments were carried out in accordance with the institutional guidelines for the use of laboratory animals. For the tumorigenesis study, tumors were formed by s.c. injecting cancer cells into nonobese diabetic/severe combined immunodeficient mice. NCI H460 cells were treated with the indicated compound at 5 μmol/L or vehicle (0.05% DMSO) for 48 hours. They were dissociated to single cells by trypsin-EDTA and resuspended in PBS for injection. Groups of mice were inoculated with 5×10^5, 5×10^4, or 5×10^3 cells in 100 μL volume. Tumor growth was monitored every 2 days. Animals were sacrificed after 4 months or until the tumor grow to >2.0 cm in diameter.

For the chemo-combination treatment study, tumors were formed by s.c. injecting 1×10^5 NCI H460 cells into the flank of *nu/nu* mouse. Treatment was started when the tumors developed to ~5 mm in diameter. Compound was injected i.p. for three times every 2 days. From the day of second compound administration, cisplatin (3 mg/kg) was injected i.p. for three times every 2 days. The day of first cisplatin administration was designated day 0, and tumor sizes were measured every 2 days thereafter. Tumor volume was calculated by the formula 0.52 × length × width^2. Most

Published OnlineFirst September 14, 2010; DOI:10.1158/0008-5472.CAN-09-4360

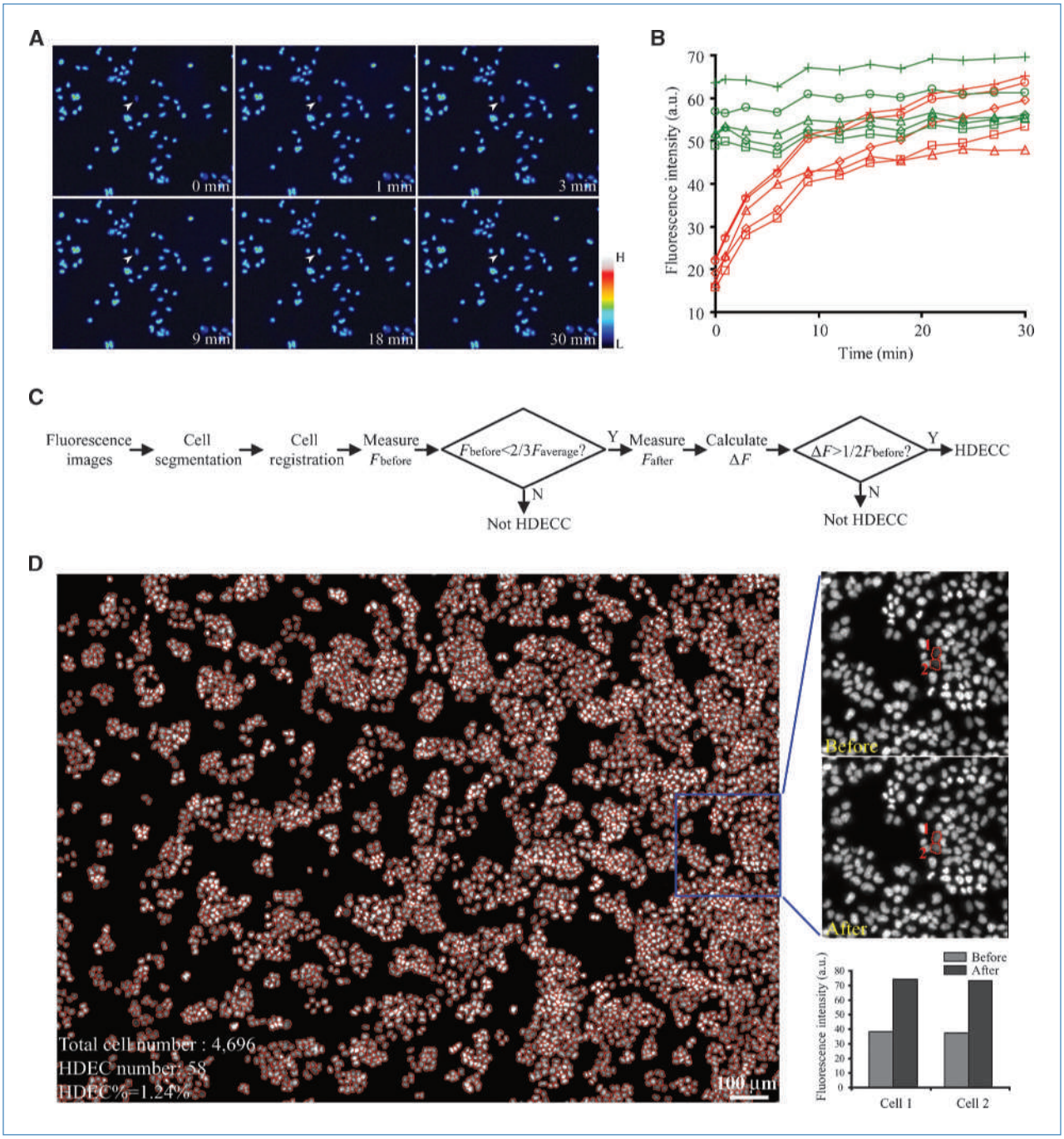

Figure 1. Development of the image-based HDECC assay. A, time-lapse imaging of the Hoechst-stained NCI H460 cells before (0 min) and during verapamil treatment. Pointed is an example of HDECC, which was dye resistant initially and brightened up when the efflux pump was blocked. B, fluorescence intensities of five random chosen examples of HDECCs (red) and non-HDECCs (green) measured by automated quantification of the time-lapse images. C, automated image analysis pipeline for HDECC identification. F_{before}, fluorescence intensity before verapamil treatment; F_{after}, fluorescence intensity 10 min after verapamil treatment; $F_{average}$, average fluorescence intensity of all the counted cells; $\Delta F = F_{after} - F_{before}$. D, an example of automatically segmented image containing 4,696 cells. Cells were circled with red lines along the segmentation boundary for fluorescence quantification. Inserted are images of two HDECCs before and 10 min after verapamil treatment. With their fluorescence intensities before and after verapamil treatment quantified in the graph below.

compound dosages were adopted from literature. The dosages were 1 mg/kg CGS-15943 (24), 5 mg/kg 8-(3-chlorostyryl) caffeine (25), 1 mg/kg fluspirilene (26), 3 mg/kg fiduxosin hydrochloride (27), 3 mg/kg fluphenazine dihydrochloride (28), 5 mg/kg SB 228357 (29), 50 mg/kg PQ 401 (30), and 3 mg/kg DMCM hydrochloride (31). PRL-3 inhibitor I has not been studied *in vivo* previously, and 10 mg/kg was used in this study.

Published OnlineFirst September 14, 2010; DOI:10.1158/0008-5472.CAN-09-4360

In vitro colony formation assay

Purified SP cells were treated with indicated compound. They were then plated at clonal density (1,250 per well) in the flat-bottomed 24-well plate. Culture medium contained 0.35% agarose to immobilize the cells. The numbers of clones formed were counted after 2 weeks.

Statistical data analysis and EC_{50} curve fitting

Data were presented as the mean ± SD. Statistical significance was analyzed by two-tailed *t* test and power analysis using Microsoft Excel software (Microsoft). *P* values of <0.05 were considered significant. To calculate EC_{50}, dose-response experiments were carried out by testing the compounds at a 10-fold dilution series from 10 nmol/L to 100 μmol/L. The averaged results of three independent experiments were used to calculate the EC_{50} values by fitting to a four-parameter (Y_{min}, Y_{max}, EC_{50}, and Hill coefficient) sigmoidal dose-response curve as follows:

$$Y = Y_{min} + \frac{Y_{max} - Y_{min}}{1 + 10^{(\log EC_{50} - X) \times (\text{Hill coefficient})}}$$

Where *X* is the logarithm of concentration and *Y* is the predicted value. Curve fitting was performed with XLFIT 5.1 software (Innovation in Research Data Management).

Results

HDECCs can be identified by fluorescence microscopy

Similar to SP assay, we used Hoechst dye as an indicator to measure the drug efflux from cancer cells. The assay was first tested on NCI H460 lung cancer cells, which have been shown to contain SP cells that are enriched with stem-like cancer cells (11). After incubating the cells with 5 μg/mL Hoechst 33342 for 90 minutes, a few dye-resistant cells were detected as indicated by the significantly lower intensity of the nuclei (Fig. 1A, 0 min). To verify that the low fluorescence is caused by drug efflux and exclude all other possibilities, 50 μmol/L verapamil was added to the medium to block the efflux pump in the presence of Hoechst dye. The treatment significantly increased the intensities of the dye-resistant cells to almost normal level within 30 minutes (Fig. 1A). In this approach, HDECCs were identified with high confidence by microscopy. Using the assay, HDECCs were detected in 11 cell lines we tested, including 8 lung cancer cell lines, 2 breast cancer cell lines, and 1 prostate cancer cell line (Table 1).

Table 1. Percentage of HDECCs in various cancer cell lines detected by the image-based assay

Cancer cell line	Cancer type	HDECC (%)
NCI H460	Lung, non–small cell	1.30
A549	Lung, non–small cell	0.88
NCI H23	Lung adenocarcinoma, non–small cell	0.75
NCI H522	Lung adenocarcinoma, non–small cell	1.12
NCI H226	Lung squamous cell carcinoma	1.62
SK-MES-1	Lung squamous cell carcinoma	1.30
NCI H2170	Lung squamous cell carcinoma	0.55
NCI H441	Lung papillary adenocarcinoma	1.15
MDA-MB-435S	Breast, duct	3.78
SK-BR-3	Breast, adenocarcinoma	1.14
Du-145	Prostate	0.9

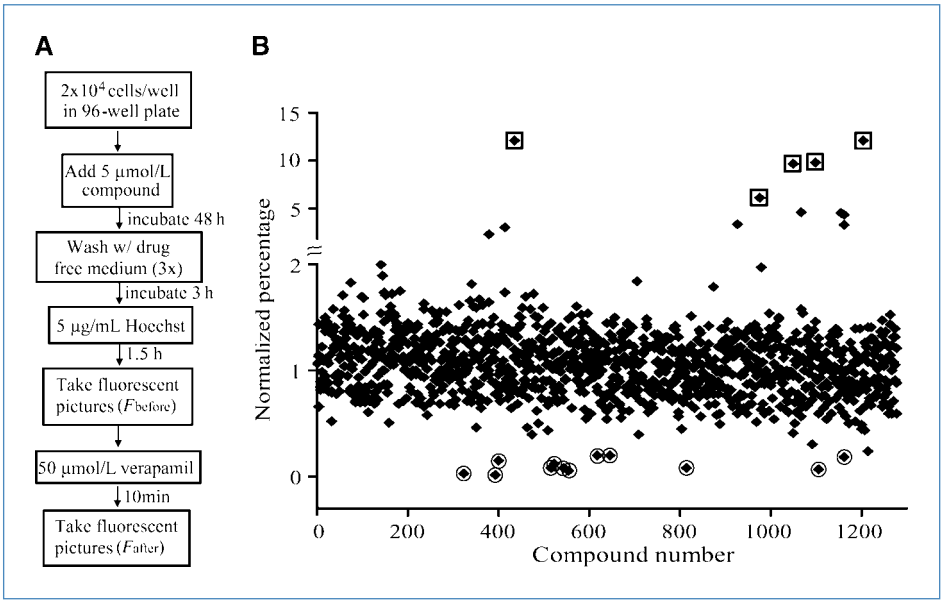

Figure 2. LOPAC screening. A, workflow of the screening procedure. B, scatter plot of the effect of all 1,280 LOPAC compounds on the percentage of HDECCs in NCI H460 cells. Results shown are the average of three experiments normalized to the control; error bars were omitted for the clarity of view. Twelve potent inhibitors (circles) were identified when the threshold for selection of hits was set at 5 SD from the mean. The screen also identified five compounds, increasing the HDECC percentage by >5-fold (squares).

Published OnlineFirst September 14, 2010; DOI:10.1158/0008-5472.CAN-09-4360

To accurately measure the percentage of HDECCs, fluorescence images were taken under a low-magnification 4× objective so that a large number of cells (~4,000) could be analyzed. For NCI H460 cells, statistical analysis showed that the result had normal distribution with an average of 1.3% and a half-width of <0.5 (Supplementary Fig. S1A). To test whether the accuracy is capable to identify HDECC effectors, SP-free cells were prepared by removing the SP cells using flow cytometry to mimic the effect of HDECC inhibitors. This significantly reduced the HDECC percentage to 0.05%, and our assay predictably detected it (Supplementary Fig. S1B). This confirmed that the HDECCs we identified

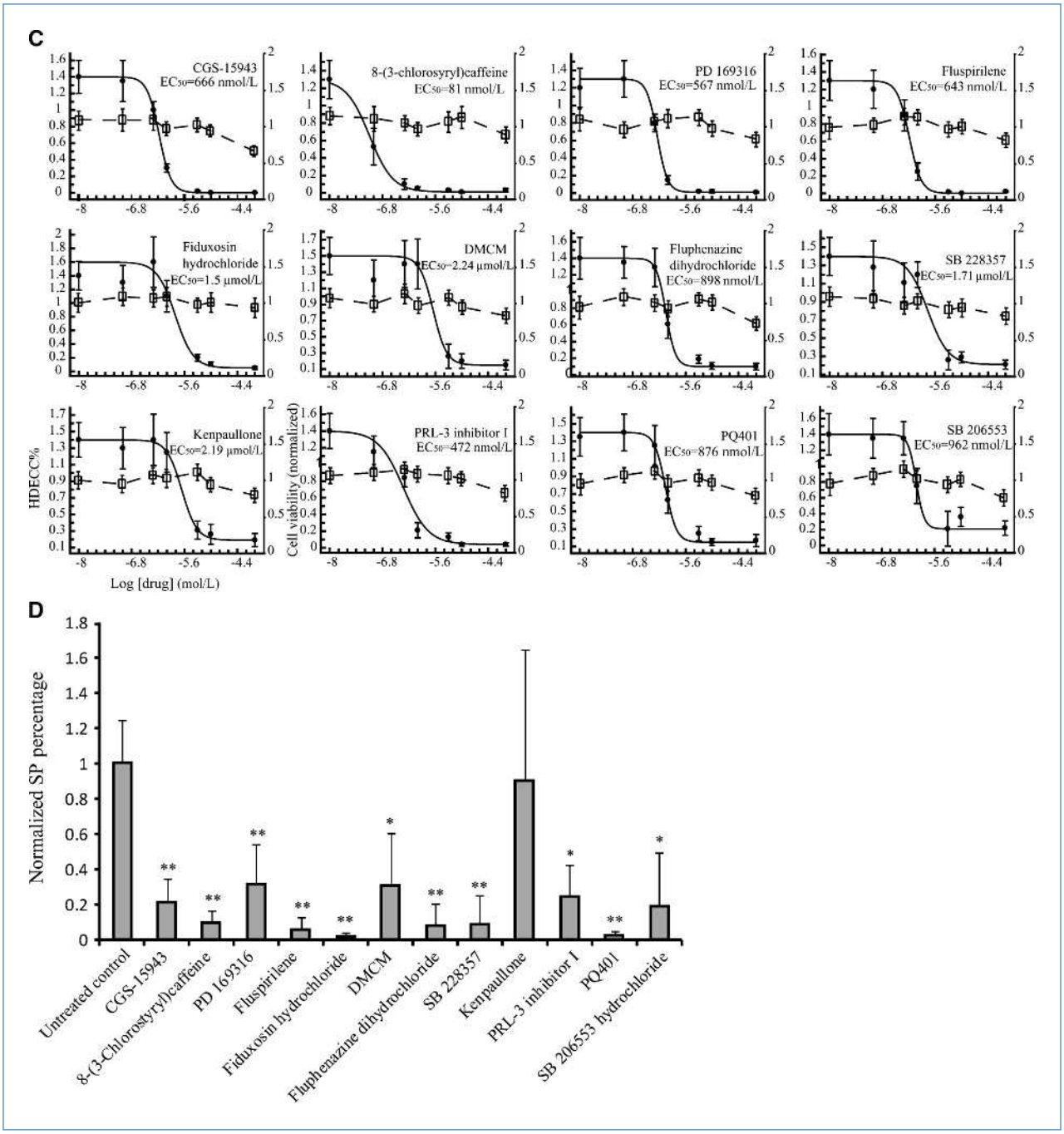

Figure 2. ***Continued.*** C, dose-response curves for the 12 inhibitors (solid lines) and their EC_{50} values. Viable cells were counted by MTS assay under each treatment condition and plotted in dot lines, and results were normalized with control set as 1. D, validation of the inhibitors by SP analysis. The percentages of SP cells were counted by flow cytometry after the treatment of indicated compound. Results shown are normalized averages of three independent experiments with indicated error bars except for Kenpaullone, which was repeated five times. *, $P < 0.05$; **, $P < 0.01$.

Published OnlineFirst September 14, 2010; DOI:10.1158/0008-5472.CAN-09-4360

Table 2. HDECC inhibitors identified by the LOPAC screening and their protein targets

Compound	Action	Protein target(s)
Fiduxosin hydrochloride	Antagonist	α1-Adrenoceptor (ADRA1)
SB 228357	Antagonist	5-HT2B/2C serotonin receptor (5-HTR)
SB 206553 hydrochloride	Antagonist	5-HT2C/5-HT2B serotonin receptor (5-HTR)
Kenpaullone	Inhibitor	Cyclin-dependent kinase (CDK)
PD 169316	Inhibitor	p38, mitogen-activated protein kinase 1 (MAPK1)
PQ401	Inhibitor	Insulin-like growth factor-I receptor (IGF-IR)
CGS-15943	Antagonist	A1 adenosine receptor (ADOR)
8-(3-Chlorostyryl)caffeine	Antagonist	A2A adenosine receptor (ADOR)
Fluphenazine dihydrochloride	Antagonist	D1/D2 dopamine receptor (DR)
Fluspirilene	Antagonist	D1/D2 dopamine receptor (DR)
PRL-3 inhibitor I	Inhibitor	Phosphatase of regenerating liver-3 (PRL-3)
DMCM	Agonist	γ-Aminobutyric acid receptor (GABR)

were equivalent to SP and the image-based assay had the capability to identify inhibitors on them.

Automated image analysis enables the image-based assay for HCS study

Regular automated fluorescence microscopes typically can acquire >10,000 images per day; the factor that limits the throughput of the image-based assay is now often the ability to process the massive image data generated (32, 33). To overcome the limit, we developed image analysis program to automatically identify HDECCs. The image stack was first aligned to correct the displacements of frames due to the drift of microscope. Cells were then detected and segmented in each image using algorithms implemented in DCellIQ software (32, 33). Then, the cells were registered to quantify the fluorescence variation (see Supplementary Materials and Methods for details). Through the automated quantification, HDECCs were distinguished from non-HDECCs as shown in Fig. 1B. Due to the marked discrepancy observed between the two populations, we simplified image analysis to use only two images to identify HDECCs so that the assay was greatly accelerated (Fig. 1C). Dull cells (initial fluorescence intensity <2/3 average) significantly brightened by verapamil treatment (ΔF >50% after 10 minutes) were designated as HDECCs. The parameters were arbitrarily set and optimized, as there is no quantitative definition of HDECCs or SP. Our results presented later showed that with the parameters, the image-based assay result is consistent with SP analysis. With the program, HDECCs were automatically identified and counted after image acquisition (Fig. 1D), so that >1,000 conditions (twelve 96-well plates) can be screened daily with a regular fluorescence microscope. This made the system feasible to conduct HCS studies.

LOPAC screening identifies HDECC inhibitors

Screening was carried out on LOPAC library, which contains 1,280 latest compounds representing all major target classes (34, 35), to identify inhibitors that can markedly reduce the number of HDECCs in NCI H460 cells. Cells were treated with 5 μmol/L of the compound for 48 hours. To exclude ABC transporter inhibitors and identify effectors inhibiting HDECCs through other mechanisms, cells were then extensively washed to remove the binding compound before the assay (Fig. 2A). Consequently, none of the known inhibitors (e.g., verapamil and cyclosporin A) was identified as screening hit, although they can markedly reduce HDECCs if the cells were not washed (data not shown).

The screening was carried out in 96-well plate format with a minimum of three replicates. Reproducibility was confirmed by Pearson correlation analysis (Supplementary Fig. S2A). The suitability of the system for high-throughput screening was also confirmed by Z′-factor test (36). Due to the lack of known HDECC inhibitor, positive controls were prepared by either removing SP cells using flow cytometry or treating cells with 5 μmol/L ABC transporter inhibitor verapamil for 48 hours and then performing the assay without washing. Z′-factors were above 0.5 using both positive controls as shown in Supplementary Fig. S2B.

Significant cytotoxicity was observed for 76 (5.9%) compounds in the screening. The cytotoxicity caused >50% reduction of total cell numbers in these wells over the time course of the assay. Cells treated with these compounds also appeared to be granule and detached from plate. The images, before and after verapamil treatment, could not be aligned as a result of the mobility of the detached cells. Therefore, these compounds were excluded from further analysis. Twelve potent inhibitors were identified in the screening when the threshold for selection of hits was set at 5 SD from the mean (Fig. 2B, red circles). These compounds and their known protein targets are listed in Table 2. To further exclude the possibility that these inhibitors simply block pump function, assays were carried out to measure HDECCs following a short-term compound treatment for 30 minutes. None of the 12 inhibitors caused significant reduction (P > 0.05) of HDECCs in this condition (Supplementary Fig. S3), confirming that the effects were achieved through long-term cellular mechanism (possibly transcriptional) instead of acutely blocking pumps. To verify the primary screening hits,

Published OnlineFirst September 14, 2010; DOI:10.1158/0008-5472.CAN-09-4360

dose-response experiments were carried out and the EC_{50} values were calculated (Fig. 2C). The result showed that these inhibitors can achieve the inhibitive effect at comparable or lower concentrations than compounds selectively killing P-glycoprotein–overexpressed MDR cells such as NSC73306 (37, 38). None of the inhibitors had significant effect on the cell viability or proliferation until 10 μmol/L (Fig. 2C), excluding the possibility that the reduction of HDECC percentage was caused by the increase of non-HDECCs. The time-lapse imaging capability of the image-based assay also allowed us

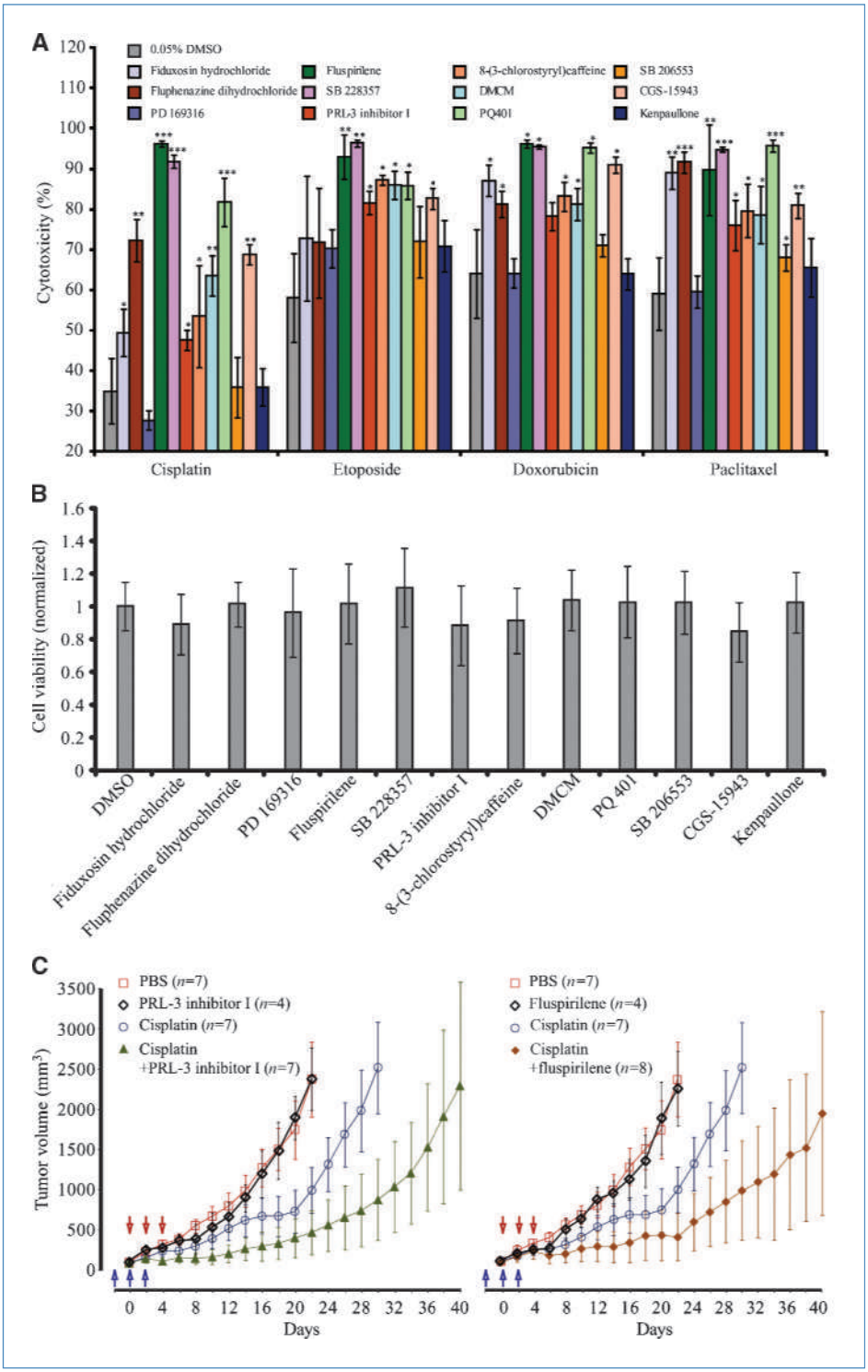

Figure 3. Enhancement of the chemotherapy efficacy by HDECC inhibitors. A, enhancement of the chemotherapeutic drug effects on SP cells *in vitro*. SP cells were purified by flow cytometry and treated with four different chemotherapeutic drugs: 100 μmol/L cisplatin, 100 μmol/L etoposide, 20 μmol/L doxorubicin, or 400 nmol/L paclitaxel, with or without the indicated compound at 5 μmol/L. Cytotoxicity was measured after 48 h using MTS assay. *, $P < 0.05$; **, $P < 0.01$; ***, $P < 0.001$. B, compound alone does not have an effect on SP cell viability as measured by MTS assay. C, compound effects on the chemotherapy efficacy *in vivo*. Significant tumor reduction was observed from day 8 for PRL-3 inhibitor I ($P < 0.05$) and day 10 for fluspirilene ($P < 0.05$) compared with cisplatin treatment alone. PRL-3 inhibitor I or fluspirilene alone did not have an effect. Arrows indicate the administration of compound (blue) and cisplatin (red).

Published OnlineFirst September 14, 2010; DOI:10.1158/0008-5472.CAN-09-4360

Table 3. Effect of HDECC inhibitors on the tumorigenicity of NCI H460 lung cancer cells

Treatment	Tumors/injections		
	5×10^5 cells/injection	5×10^4 cells/injection	5×10^3 cells/injection
DMSO (control)	5/5	6/6	5/6
Fiduxosin hydrochloride		5/5	5/5
SB 228357		5/5	5/5
SB 206553 hydrochloride		5/5	5/6
Kenpaullone		5/5	4/4
PD 169316		5/5	4/5
PQ401		5/5	4/5
CGS-15943		5/5	5/6
8-(3-Chlorostyryl)caffeine		5/5	4/5
Fluphenazine dihydrochloride	5/5	5/5	6/11* (P = 0.044, power = 0.998)
Fluspirilene	5/5	4/5	3/9* (P = 0.002, power = 0.999)
PRL-3 inhibitor I	5/5	4/5	4/10* (P = 0.008, power = 0.999)
DMCM	5/5	5/5	4/10* (P = 0.008, power = 0.999)

*, $P < 0.05$.

to test whether the inhibitors can directly kill HDECCs. The result showed that HDECCs survived the treatment of all the 12 inhibitors based on bright-field inspection. However, their drug efflux capability was significantly impaired by the treatment (Supplementary Fig. S4). Overall, the screening identified 12 nontoxic compounds that can potently inhibit the drug efflux capability of HDECCs through mechanism other than blocking ABC transporters.

When the threshold for selection of hits was lowered to 3 SD from the mean, additional 12 compounds were identified as screening hits. Many of the effective compounds share the same protein targets (e.g., three inhibitors are dopamine receptor antagonists). It is surprising that the effects of the compounds on lung cancer cells are achieved through neurotransmitter receptors. However, our Western blot result showed that indeed D1 and D2 dopamine receptors were expressed in the lung cancer cell lines (Supplementary Fig. S5). The exact molecular mechanism underlying the compound effects still remains to be studied. Interestingly, the screening also identified five compounds that can markedly increase the HDECC percentage by >5-fold, such as retinoic acid and its analogue TTNPB (Fig. 2B, blue squares). A complete list of the screening results is shown in Supplementary Table S1.

HDECC inhibitors are capable of inhibiting SP

SP analysis was carried out to further validate the assay and confirm screening hits. NCI H460 cells were treated with 5 μmol/L of the compound for 48 hours and sorted by flow cytometry. A representative dot plot from triplet experiment for each inhibitor is shown in Supplementary Fig. S6. The average percentage of SP cells was normalized (control set as 1) and plotted in Fig. 2D. Significant inhibition of SP was achieved for all the inhibitors except Kenpaullone, for which large variation among experiments was observed. This strongly supported that the HDECCs identified by the image-based assay were identical to SP and the system we established can be used reliably to identify inhibitors on them.

HDECC inhibitors increase the efficacy of chemotherapy *in vitro* and *in vivo*

HDECCs are significant obstacles for chemotherapy as they cause MDR. We next tested whether the inhibitors may help to overcome this obstacle by sensitizing HDECCs to chemotherapeutic drugs. Our result first showed that indeed HDECCs were significantly more resistant to four commonly used chemotherapeutic drugs (cisplatin, etoposide, doxorubicin, and paclitaxel) compared with the unsorted whole cancer cell population (Supplementary Fig. S7; ref. 11). Nine of the 12 inhibitors successfully reversed the drug resistance and enabled much more HDECCs to be killed *in vitro* (Fig. 3A) by the coadministered chemotherapeutic drugs. When these compounds were administered alone, no significant cytotoxicity was observed on the HDECCs purified as SP cells (Fig. 3B), which is consistent with the time-lapse cell tracking results (Supplementary Fig. S4). The sensitization effect was universal for the four structurally dissimilar and functionally divergent drugs, confirming the capability of the inhibitors to remove MDR. This result suggests that the reported system may provide a new tool for drug discovery to treat MDR, which has been a major goal for cancer biologists for decades (5).

The nine compounds that can enhance the efficacy of chemotherapy *in vitro* were further tested *in vivo* using a xenografted animal model. Compounds were administered in combination with cisplatin at dosages indicated in Materials and Methods. Animals that received fiduxosin hydrochloride became moribund so that the experiment was terminated according to institutional animal use guideline. No significant effects were observed for six compounds (Supplementary Fig. S8) compared with animals receiving cisplatin treatment alone. The

Published OnlineFirst September 14, 2010; DOI:10.1158/0008-5472.CAN-09-4360

remaining two compounds (PRL-3 inhibitor I and fluspirilene) significantly enhanced the chemotherapy efficacy, which further inhibited tumor growth compared with cisplatin alone ($P < 0.05$ after day 8 for PRL-3 inhibitor I and after day 10 for fluspirilene; Fig. 3C).

HDECC inhibitors reduce the tumorigenicity of lung cancer cells

In light of the evidences that HDECCs may be highly enriched with stem-like cancer cells, we sought to test whether the HDECC inhibitors can also inhibit stem-like cancer cells. Animal transplant experiments were carried out to assess the *in vivo* tumor formation ability of NCI H460 cells after compound treatment *in vitro* for 48 hours. For control cells treated with DMSO, all the injections result in tumor formation when $>5 \times 10^4$ cells were injected, and most (five of six) injections formed tumor at 5×10^3 cells per dosage. When the cells were treated with the inhibitors, no significant effects were observed for eight compounds (Table 3). Interestingly, four of the compounds (fluphenazine dihydrochloride, fluspirilene, PRL-3 inhibitor I, and DMCM) decreased the tumor formation incidence when 5×10^3 cells were injected. None of the reduction was complete because the treated cells still formed tumors in some injections. However, compared with the groups of compounds that did not show effect, the reductions caused by these four inhibitors were statistically significant (Table 3). These compounds were also shown to be able to reduce the colony formation capability of purified SP cells *in vitro* by the agarose colony formation assay (Supplementary Fig. S9). These results suggest that the four compounds may directly interfere with the function of stem-like cancer cells. The results also support that there is direct correlation between the HDECC population and the stem-like cancer cell population, which has been controversial, although it is supported by more and more emerging evidence. Fluphenazine dihydrochloride and DMCM were not effective in the above-mentioned *in vivo* chemo-combination treatment study. This is possibly caused by limited compound accessibility to tumor cells *in vivo* or poor pharmacokinetics and pharmacodynamics of the compounds, which remain to be studied.

Discussion

In this study, we developed an image-based assay to specifically analyze the HDECC population in cancer cells. The assay can be easily adopted for high-throughput studies using a regular automated fluorescence microscope. This capability was shown by a screening on the LOPAC library, which successfully identified 12 compounds that can potently inhibit HDECCs in lung cancer cells. Our study focused on lung cancer cells, but the assay can also be performed on adherent cancer cells of other origins (Table 1).

The nature of HDECCs is still unclear. Many recent studies showed that they are more tumorigenic when injected into immunodeficient mice, suggesting that they are selectively enriched with stem-like cancer cells (6–14). Whether there is correlation between the two cell populations remains controversial, and our results that four compounds inhibiting HDECCs reduced the tumorigenicity of cancer cells provided new evidence for this correlation. Moreover, several proteins targeted by the inhibitors identified in this work have been shown by independent studies to play key roles in stem-like cancer cells. One of the targets, PRL-3, has been associated with tumorigenesis and metastasis by many studies (39, 40). Compounds modulating the other target, dopamine receptor, can potently inhibit the growth of cancerous neural progenitor cells (35). These evidences support an effect of the HDECC inhibitors on stem-like cancer cells and a relationship between HDECCs and stem-like cancer cells. However, it should be noted that none of the inhibition of tumorigenicity was complete, possibly because the two cell populations are not identical, although highly overlapping. Drug screening on cancer stem cells is challenging due to the rarity of these cells as well as their instability in culture such that few advances have been made thus far (41), and the current reported system may provide a new angle for cancer stem cell research and drug discovery.

In addition to their correlation with stem-like cancer cells, HDECCs represent a major obstacle for chemotherapy as they cause MDR. Traditionally, development of drugs to overcome resistance has been done on induced resistant cell lines generated by continuous or pulsed exposure to drugs (42, 43). However, such induced cells often are associated with changes that are partly characteristic of resistance to certain drugs instead of MDR (44). We adopted a different approach by selectively studying an intrinsic MDR cell population in the context of the whole cancer cell population. Nine compounds were identified by the reported HCS system that can nonspecifically enhance the efficacy of chemotherapeutic drugs *in vitro*, and two of them were further shown to be also effective *in vivo* (Fig. 3), highlighting its potential for MDR drug discovery. However, MDR can be caused by a huge variety of transporters and many of them may not be revealed by the Hoechst efflux assay, as well as mechanisms other than drug efflux (5), so that ineffective compounds may be identified in our screening. Indeed, three inhibitors failed to improve chemotherapy efficacy either *in vitro* or *in vivo*, although they were able to reduce Hoechst efflux. Nevertheless, most inhibitors identified significantly improved the efficacy for all the chemotherapy drugs we tested at least *in vitro*, suggesting that Hoechst efflux may be used as an effective indicator for MDR. None of the effective inhibitors kill HDECCs directly, and our system was able to identify these nontoxic effectors because the image-based approach allowed more comprehensive measurement of the responses to perturbance than simple viability assay. Our study focused on drug efflux and cell viability, but actually a complete morphology phenotype profile can be generated from the images (22), which may greatly facilitate related mechanism study in the future.

High-throughput compound library screening usually identifies effectors that result in desired phenotype without revealing their mechanism. In the absence of the knowledge, it is hard to predict the therapeutic potential of the compounds as they may be associated with severe side effects.

Published OnlineFirst September 14, 2010; DOI:10.1158/0008-5472.CAN-09-4360

For this concern, we used LOPAC library, of which the compound has been extensively characterized with known protein-substrate interactions. Such approach may not only allow quick translation of the screening result to clinical application but also reveal the "chemical genetics" (45) to provide insight into the related molecular mechanisms. The latter potential is shown by the consistency of our screening results with previous reports on individual protein targets, like the aforementioned roles of dopamine receptor and PRL-3 for stem-like cancer cells. Reduction of HDECC by the insulin-like growth factor-I receptor (IGF-IR) inhibitor PQ401 is also consistent with previous reports that IGF-IR inhibition may sensitize lung cancer cells to chemotherapy (46), suggesting a key role of IGF-IR for MDR. The finding that retinoic acid can significantly increase HDECC is surprising, but retinoic acid has long been noticed to be able to induce the expression of MDR genes and cause drug resistance (47, 48), although it has been used clinically for leukemia treatment to induce stem cell differentiation. Other mechanisms, such as the reduction of tumorigenicity by DMCM, are unclear and need to be further investigated. With a more complete library with most major signaling pathways targeted by multiple structurally divergent chemicals, such chemical genetics approach would help to reveal the whole repertoire of signaling pathways underlying HDECCs.

Disclosure of Potential Conflicts of Interest

No potential conflicts of interest were disclosed.

Grant Support

This work was supported by NIH grant U54CA149196 (S. Wong).

The costs of publication of this article were defrayed in part by the payment of page charges. This article must therefore be hereby marked *advertisement* in accordance with 18 U.S.C. Section 1734 solely to indicate this fact.

Received 11/30/2009; revised 06/24/2010; accepted 06/26/2010; published OnlineFirst 09/14/2010.

References

1. Chen CJ, Chin JE, Ueda K, et al. Internal duplication and homology with bacterial transport proteins in the mdr1 (P-glycoprotein) gene from multidrug-resistant human cells. Cell 1986;47:381–9.
2. Zhou S, Schuetz JD, Bunting KD, et al. The ABC transporter Bcrp1/ABCG2 is expressed in a wide variety of stem cells and is a molecular determinant of the side-population phenotype. Nat Med 2001;7:1028–34.
3. Baer MR, George SL, Dodge RK, et al. Phase 3 study of the multidrug resistance modulator PSC-833 in previously untreated patients 60 years of age and older with acute myeloid leukemia: Cancer and Leukemia Group B Study 9720. Blood 2002;100:1224–32.
4. Nobili S, Landini I, Giglioni B, Mini E. Pharmacological strategies for overcoming multidrug resistance. Curr Drug Targets 2006;7:861–79.
5. Szakacs G, Paterson JK, Ludwig JA, Booth-Genthe C, Gottesman MM. Targeting multidrug resistance in cancer. Nat Rev Drug Discov 2006;5:219–34.
6. Wulf GG, Wang RY, Kuehnle I, et al. A leukemic stem cell with intrinsic drug efflux capacity in acute myeloid leukemia. Blood 2001;98:1166–73.
7. Hirschmann-Jax C, Foster AE, Wulf GG, et al. A distinct "side population" of cells with high drug efflux capacity in human tumor cells. Proc Natl Acad Sci U S A 2004;101:14228–33.
8. Chiba T, Kita K, Zheng YW, et al. Side population purified from hepatocellular carcinoma cells harbors cancer stem cell-like properties. Hepatology 2006;44:240–51.
9. Haraguchi N, Utsunomiya T, Inoue H, et al. Characterization of a side population of cancer cells from human gastrointestinal system. Stem Cells 2006;24:506–13.
10. Szotek PP, Pieretti-Vanmarcke R, Masiakos PT, et al. Ovarian cancer side population defines cells with stem cell-like characteristics and Mullerian inhibiting substance responsiveness. Proc Natl Acad Sci U S A 2006;103:11154–9.
11. Ho MM, Ng AV, Lam S, Hung JY. Side population in human lung cancer cell lines and tumors is enriched with stem-like cancer cells. Cancer Res 2007;67:4827–33.
12. Wang J, Guo LP, Chen LZ, Zeng YX, Lu SH. Identification of cancer stem cell-like side population cells in human nasopharyngeal carcinoma cell line. Cancer Res 2007;67:3716–24.
13. Wu C, Wei Q, Utomo V, et al. Side population cells isolated from mesenchymal neoplasms have tumor initiating potential. Cancer Res 2007;67:8216–22.
14. Engelmann K, Shen H, Finn OJ. MCF7 side population cells with characteristics of cancer stem/progenitor cells express the tumor antigen MUC1. Cancer Res 2008;68:2419–26.
15. Al-Hajj M, Wicha MS, Benito-Hernandez A, Morrison SJ, Clarke MF. Prospective identification of tumorigenic breast cancer cells. Proc Natl Acad Sci U S A 2003;100:3983–8.
16. Singh SK, Hawkins C, Clarke ID, et al. Identification of human brain tumour initiating cells. Nature 2004;432:396–401.
17. Kim CF, Jackson EL, Woolfenden AE, et al. Identification of bronchioalveolar stem cells in normal lung and lung cancer. Cell 2005;121:823–35.
18. Goodell MA, Brose K, Paradis G, Conner AS, Mulligan RC. Isolation and functional properties of murine hematopoietic stem cells that are replicating *in vivo*. J Exp Med 1996;183:1797–806.
19. Conrad C, Erfle H, Warnat P, et al. Automatic identification of subcellular phenotypes on human cell arrays. Genome Res 2004;14:1130–6.
20. Perlman ZE, Slack MD, Feng Y, Mitchison TJ, Wu LF, Altschuler SJ. Multidimensional drug profiling by automated microscopy. Science 2004;306:1194–8.
21. Tanaka M, Bateman R, Rauh D, et al. An unbiased cell morphology-based screen for new, biologically active small molecules. PLoS Biol 2005;3:e128.
22. Loo LH, Wu LF, Altschuler SJ. Image-based multivariate profiling of drug responses from single cells. Nature Methods 2007;4:445–53.
23. Giuliano KA, DeBiasio RL, Dunlay RT, et al. High-content screening: a new approach to easing key bottlenecks in the drug discovery process. J Biomol Screen 1997;2:249–59.
24. Holtzman SG. CGS 15943, a nonxanthine adenosine receptor antagonist: effects on locomotor activity of nontolerant and caffeine-tolerant rats. Life Sci 1991;49:1563–70.
25. Jacobson KA, Nikodijevic O, Padgett WL, Gallo-Rodriguez C, Maillard M, Daly JW. 8-(3-Chlorostyryl)caffeine (CSC) is a selective A2-adenosine antagonist *in vitro* and *in vivo*. FEBS Lett 1993;323:141–4.
26. Pedata F, Sorbi S, Pepeu G. Choline high-affinity uptake and metabolism and choline acetyltransferase activity in the striatum of rats chronically treated with neuroleptics. J Neurochem 1980;35:606–11.
27. Brune ME, Katwala SP, Milicic I, et al. Effect of fiduxosin, an antagonist selective for α(1A)- and α(1D)-adrenoceptors, on intraurethral and arterial pressure responses in conscious dogs. J Pharmacol Exp Ther 2002;300:487–94.
28. Aravagiri M, Marder SR, Yuwiler A, Midha KK, Kula NS, Baldessarini RJ. Distribution of fluphenazine and its metabolites in brain regions and other tissues of the rat. Neuropsychopharmacology 1995;13:235–47.

Published OnlineFirst September 14, 2010; DOI:10.1158/0008-5472.CAN-09-4360

29. Reavill C, Kettle A, Holland V, Riley G, Blackburn TP. Attenuation of haloperidol-induced catalepsy by a 5-HT2C receptor antagonist. Br J Pharmacol 1999;126:572–4.
30. Gable KL, Maddux BA, Penaranda C, et al. Diarylureas are small-molecule inhibitors of insulin-like growth factor I receptor signaling and breast cancer cell growth. Mol Cancer Ther 2006;5:1079–86.
31. Leppa E, Vekovischeva OY, Linden AM, et al. Agonistic effects of the β-carboline DMCM revealed in GABA(A) receptor γ2 subunit F77I point-mutated mice. Neuropharmacology 2005;48:469–78.
32. Chen X, Zhou X, Wong ST. Automated segmentation, classification, and tracking of cancer cell nuclei in time-lapse microscopy. IEEE Trans Biomed Eng 2006;53:762–6.
33. Wang M, Zhou X, Li F, Huckins J, King RW, Wong ST. Novel cell segmentation and online SVM for cell cycle phase identification in automated microscopy. Bioinformatics 2008;24:94–101.
34. Rodgers G, Hubert C, McKinzie J, et al. Development of displacement binding and GTPγS scintillation proximity assays for the identification of antagonists of the micro-opioid receptor. Assay Drug Dev Technol 2003;1:627–36.
35. Diamandis P, Wildenhain J, Clarke ID, et al. Chemical genetics reveals a complex functional ground state of neural stem cells. Nat Chem Biol 2007;3:268–73.
36. Zhang JH, Chung TD, Oldenburg KR. A simple statistical parameter for use in evaluation and validation of high throughput screening assays. J Biomol Screen 1999;4:67–73.
37. Hall MD, Salam NK, Hellawell JL, et al. Synthesis, activity, and pharmacophore development for isatin-β-thiosemicarbazones with selective activity toward multidrug-resistant cells. J Med Chem 2009;52:3191–204.
38. Turk D, Hall MD, Chu BF, et al. Identification of compounds selectively killing multidrug-resistant cancer cells. Cancer Res 2009;69:8293–301.
39. Saha S, Bardelli A, Buckhaults P, et al. A phosphatase associated with metastasis of colorectal cancer. Science 2001;294:1343–6.
40. Stephens BJ, Han H, Gokhale V, Von Hoff DD. PRL phosphatases as potential molecular targets in cancer. Mol Cancer Ther 2005;4:1653–61.
41. Gupta PB, Onder TT, Jiang G, et al. Identification of selective inhibitors of cancer stem cells by high-throughput screening. Cell 2009;138:645–59.
42. Keizer HG, Schuurhuis GJ, Broxterman HJ, et al. Correlation of multidrug resistance with decreased drug accumulation, altered subcellular drug distribution, and increased P-glycoprotein expression in cultured SW-1573 human lung tumor cells. Cancer Res 1989;49:2988–93.
43. Zaman GJ, Versantvoort CH, Smit JJ, et al. Analysis of the expression of MRP, the gene for a new putative transmembrane drug transporter, in human multidrug resistant lung cancer cell lines. Cancer Res 1993;53:1747–50.
44. Shen DW, Cardarelli C, Hwang J, et al. Multiple drug-resistant human KB carcinoma cells independently selected for high-level resistance to colchicine, adriamycin, or vinblastine show changes in expression of specific proteins. J Biol Chem 1986;261:7762–70.
45. Walsh DP, Chang YT. Chemical genetics. Chem Rev 2006;106:2476–530.
46. Warshamana-Greene GS, Litz J, Buchdunger E, Garcia-Echeverria C, Hofmann F, Krystal GW. The insulin-like growth factor-I receptor kinase inhibitor, NVP-ADW742, sensitizes small cell lung cancer cell lines to the effects of chemotherapy. Clin Cancer Res 2005;11:1563–71.
47. Ferrandis E, Benard J. Retinoic acid and forskolin activate the human MDR1 gene promoter in differentiated neuroblasts. Prog Clin Biol Res 1994;385:103–10.
48. Tokura Y, Shikami M, Miwa H, et al. Augmented expression of P-gp/multi-drug resistance gene by all-trans retinoic acid in monocytic leukemic cells. Leuk Res 2002;26:29–36.